ROADSIDE DISTANCE-SAMPLING SURVEYS OF WHITE-TAILED DEER IN SOUTHERN MINNESOTA (2018-2019)

John Giudice, Brian Haroldson, Tyler Obermoller, and Eric Michel

SUMMARY OF FINDINGS

This project was designed to evaluate the feasibility of using roadside distance-sampling surveys to generate a reliable and cost-effective population monitoring metric for white-tailed deer (*Odocoileus virginianus*) in Minnesota's farmland zone. Here we report on results from the 2018 and 2019 surveys. Our study area included 4 deer permit areas (DPAs = 252, 253, 296, and 299) in southern Minnesota's farmland zone. We used a geographic information system (GIS) to classify land-cover polygons into high and low strata based upon expected deer density. As part of this exercise, we evaluated 2 buffer sizes (250 and 500 m) around potential deer cover (woodland cover, permanent to semi-permanent grasslands, and wetland cover) to delineate high-density polygons. We then overlaid the study area with a hexagonal grid (size = 36.1 mi^2), which served as our primary sampling unit (PSU). We randomly selected a spatially balanced sample of 15 PSUs and used a GIS to identify all secondary roads within each PSU. We then classified each road segment based on their juxtaposition to deer-density polygons (low, high). Finally, we randomly selected road segments (secondary sampling units) using an equal allocation of effort by stratum, which generated ~200 survey miles per stratum. We surveyed each PSU 2–4 times/year in spring and based the start of the survey season on anecdotal information on spring dispersal of deer. We began surveys approximately 1 hour after sunset and we surveyed 1–2 PSUs per night. We conducted surveys with 2-member crews using hand-held infrared sensors. For each deer group (≥1 animal) detected, the survey team recorded perpendicular sighting distance, group size, and covariate information. In 2018, we collected survey data using the 250-m buffer design and used a post-hoc simulation to evaluate the 500-m buffer design. In 2019, we collected survey data using both the existing 250-m design plus a new 500-m design. Within the latter, we generated separate secondary sampling units (road segments) and conducted independent surveys within a subset of 10 PSUs. The approach used in 2019 allowed us to disentangle the effects of buffer size and secondary-sample allocation, which is important for guiding future design considerations. The best-supported distance-sampling models for the 250-m buffer design generated similar estimates of mean deer density in 2018 (8.2 deer/mi^2; 95% CI = 5.8–11.7) and 2019 (8.0 deer/mi^2; 95% CI = 5.7–11.3). Likewise, the distance model based on the 500-m buffer design generated a similar estimate of mean deer density in 2019 (8.5 deer/mi^2; 95% CI = 5.5–13.2). These density estimates were slightly higher than the 2018-19 and 2019-20 winter aerial-survey estimates (6.5 deer/mi^2, 95% CI = 4.9–8.1; 6.5 deer/mi^2, 95% CI = 5.1–7.9, respectively), which is consistent with findings that distance-sampling estimates tend to be positively biased. However, from a management perspective, the point estimates were reasonably similar. Furthermore, annual variation in distance-sampling estimates was small (albeit we only have 2 years of data) and most (>80%) of the variation in replicate counts was due to among-PSU differences rather than day-to-day variation in the observation process. Finally, the poor precision of our distance-sampling estimates is worth noting, but we could address this through

design modifications. The simplest modification would be to increase the sample of PSUs from 15 to 25, but only conduct a single survey/year, which should produce, on average, estimates with precision similar to our aerial surveys (i.e., CV ≈ 13%). Design choices related to the buffer size and secondary-sample allocation are more complicated, but similar point estimates and precision would likely be obtained with 1) a 250-m buffer and 50:50 sample allocation (low:high) or 2) a 500-m buffer with 35:65 allocation. Another year of data collection with consistent protocols in the same study area will be helpful for evaluating the ultimate question of whether a distance-sampling metric can be effectively and reliably used to help monitor white-tailed deer populations in Minnesota's farmland zone.

INTRODUCTION

White-tailed deer (*Odocoileus virginianus*) hunting-season recommendations should use the most reliable information available to determine the status of the deer population relative to goal. In Minnesota, estimates of deer abundance and trends are used to inform annual deer season-setting recommendations for each deer permit area (DPA). The primary source of information used by the Minnesota Department of Natural Resources (MNDNR) to inform decision-making is a harvest-based population model. Currently, the MNDNR collects annual data on winter severity, hunter-reported harvest, and hunter effort (license sales) at the DPA scale. Reliability of harvest-based models can be improved by incorporating annual information on spatial and temporal variation in vital rates and other model parameters. However, collection of such data is generally cost-prohibitive, especially at the DPA scale.

An alternative approach would be to collect independent recurrent information on population abundance or trends, which could be used to calibrate the population model. For example, the MNDNR has used winter aerial surveys to calibrate harvest model estimates. However, financial, logistical, and environmental (e.g., snow cover, conifer cover) constraints prevent recurrent use of aerial surveys for all DPAs. Moreover, comparisons involving aerial surveys may not be reliable in DPAs where seasonal migration is suspected to violate closure assumptions (e.g., when comparing winter surveys to harvest-based population models). Thus, alternative, cost-effective, large-scale monitoring methods are needed. One potential approach in the farmland zone is road-based distance-sampling surveys.

Road-based surveys (e.g., spotlight, thermal imaging) are commonly used by managers for deer population monitoring (McCullough 1982, Mitchell 1986, Focardi et al. 2001, Collier et al. 2007, DeYoung 2011, Kaminski et al. 2019). Unfortunately, the counting process can be highly variable in roadside surveys, possibly as a function of variation in deer distribution and resource use, which has limited the reliability of roadside indices. Applying distance-sampling methods (Buckland et al. 1993, 2004) to road-based surveys might provide a means to calibrate the counting process and make annual comparisons more reliable. However, some important statistical issues remain (Anderson et al. 1979, Burnham et al. 1980, Marques et al. 2010, McShea et al. 2011). For example, convenience sampling violates the assumption that transects are randomly placed (or that animals are randomly located with respect to transects), which can make it difficult to obtain unbiased estimates of abundance via distance-sampling theory. However, if that bias is relatively small and constant, then road-based distance-sampling surveys may still provide a reasonable index for population monitoring, calibrating the existing MNDNR population model, or as part of an integrated population model (IPM).

OBJECTIVE

Our objective was to evaluate the feasibility of using roadside distance-sampling surveys to generate a reliable (potentially biased but reasonably precise and repeatable) and cost-effective population monitoring metric for white-tailed deer in Minnesota's farmland zone.

METHODS

Study Area and Sampling Design

2018 (250-m buffer surveys)

The 7,218-km^2 study area consisted of 4 DPAs (252, 253, 296, and 299) in southern Minnesota (Figure 1A). We used a geographic information system (GIS; ArcGIS v. 10.4, Environmental Systems Research Institute, Inc., Redlands, CA) to stratify land-cover within the sampling frame into high and low strata based upon expected deer density. We defined high-density polygons as being within a 250-m buffer of woodland, grassland (permanent to semi-permanent, excluding pasture), and wetland cover classes. Low-density polygons were the remaining areas (e.g., agricultural land, open water, and urban/developed areas). Data sources for deer-density polygons included Minnesota Land Cover Classification and Impervious Surface Area by Landsat and Lidar: 2013 update – Version 2 (woodlands), a compilation of public/private grassland layers (e.g., Waterfowl Production Areas, Wildlife Management Areas, conservation easements, etc.), and the National Wetlands Inventory for Minnesota (wetlands). We then overlaid the sampling frame with a hexagonal grid, with township-sized hexagons (size = 36.1 mi^2) having >50% of their area inside the sampling frame serving as our primary sampling units (PSUs). We chose this size because it represented the approximate area that could be surveyed within a 4–6 hour period each night. We randomly selected a spatially balanced sample (Stevens and Olsen 2004) of 16 PSUs, but discarded 1 PSU that contained the city of Mankato but few rural roads. Thus, our final design contained 15 PSUs (Figure 1A). We then used a GIS to identify all secondary (e.g., county and township) roads within each PSU, defined by juxtaposition to deer-density strata (low, high). Finally, we randomly selected road segments (pooling roads >0.25 miles from all PSUs) using an equal allocation of effort by stratum (~200 miles per stratum). Thus, each PSU contained a combination of low- and high-strata road segments. We derived road data from the Roads of Minnesota, 2012 database. For the purposes of the pilot study, we were interested in obtaining sufficient observations in the low stratum to make informed decisions about the detection process and the potential to modify the stratification and allocation scheme.

2019 (250- and 500-m buffer surveys)

In 2019, we used 2 sampling frames. In addition to the existing 250-m stratification scheme described above, we also generated a 500-m stratification scheme by defining high-density polygons as being within a 500-m buffer of potential deer cover (woodland, grassland, and wetland cover classes; Figure 1B). As before, low-density polygons were the remaining areas (e.g., agricultural land, open water, and urban/developed areas). Within this new design, we retained 10 of 15 PSUs, but selected new secondary road segments. We duplicated all remaining design aspects from 2018. We added this second design to determine whether precision of the population estimate might be improved by modifying the stratification scheme.

Field Protocols

We surveyed each PSU 2–4 times, with survey dates being close in time within a PSU (i.e., variation in survey dates was greater among than within PSUs). We did this because we were primarily interested in day-to-day variation in counts and wanted to separate this from variation in counts among PSUs and over the extended survey season. We based the start of the survey season on anecdotal information on spring dispersal of deer (from wintering areas to spring-summer-fall range). To be consistent among years and to match the “modeled population”, it was important that deer were on their spring-summer-fall range. We began surveys approximately 1 hour after sunset and we surveyed 1–2 PSUs per night. We conducted surveys with 2-member crews (driver and observer) using extended-cab pickup trucks. We

detected deer using FLIR Scout III (FLIR Systems, Inc., Wilsonville, OR) hand-held infrared (IR) sensors attached to the rear windows of the vehicle with window mounts. We viewed images on dual computer monitors attached to the front passenger seat using customized mounts. The vehicle's electrical system supplied power to the monitors. The observer searched for deer along both sides of the survey route within each PSU. We initially oriented sensors at 45- and 315-degree angles from the direction of travel, but we adjusted them as needed to account for visual obstruction due to variable terrain, woody cover, buildings, etc. Survey speed ranged from 8–48 km/hour depending upon vegetative cover density. When we identified a deer group (≥1 individual), the observer directed the driver to an approximate perpendicular angle (i.e., 90 or 270 degrees) from the group to minimize sighting distance and counted group size. Then, while the observer shined the animal(s) with a spotlight, the driver measured distance and angle to the group using a laser rangefinder and digital protractor, respectively. We used a real-time, moving-map software program (DNRSurvey; Haroldson et al. 2015), coupled to a global positioning system receiver and convertible tablet computer, to guide route navigation and record survey metrics (e.g., PSU, run [survey replicate], deer and vehicle location, distance, bearing, count, cover type) to GIS shapefiles. Cover type designations included woodland, wetland, grassland, pasture, standing crop, harvested crop, other, and unknown classes. We recorded weather data (temperature, wind speed, cloud cover, precipitation) at the beginning, middle, and end of each survey route.

During the winters of 2018-19 and 2019-20, we also conducted helicopter surveys of the study area using a quadrat-based design, where quadrats were delineated by Public Land Survey (PLS) section (259 ha) boundaries. We stratified quadrats into 3 density categories (low, medium, high) using the local wildlife manager's knowledge of deer abundance and distribution. Using optimal allocation, we randomly selected a spatially balanced sample (Stevens and Olsen 2004) of 160 plots to survey. Within each plot, a pilot and 2 observers searched for deer along transects spaced 270-m intervals until they were confident all available deer were observed. To maximize sightability, we completed surveys when snow cover measured ≥15 cm and we varied survey intensity as a function of cover and deer numbers (Gasaway et al. 1986).

Data Analysis

Data truncation

A useful rule of thumb in distance sampling is to right truncate at least 5% of the data for robust estimation of the detection function (Buckland et al. 1993:106). The 95th percentile of our distance data was 284 m in 2018 and 327 m in 2019 (250-m and 500-m buffer surveys combined). We set the truncation distance w = 300 m, which resulted in 3.7% and 6.4% of the data being truncated in 2018 and 2019, respectively. We also considered left truncation because the peak in observation distances was consistently away from the road (Figure 2). However, the peak likely reflects road avoidance rather than animal movement (e.g., due to disturbance, which is unlikely in this case because crews used IR sensors for initial detection). Thus, left-truncation methods would not resolve the underlying issue that animals are not randomly distributed with respect to the transect line. Left-truncation at some distance x from the road (e.g., 100 m), with rescaling, would improve model fit by creating the desired shoulder at distance zero. However, one would then need to generate a separate ad hoc estimate of abundance for the sampling space that is within distance x of the road transect. Thus, for this pilot-study application, it seemed prudent to set left truncation = 0 and focus on evaluating the consistency of the detection function g(x). Although the resulting density estimate is likely biased (Stainbrook 2011, Marques et al. 2013), it may still serve as a useful monitoring index if the bias is reasonably consistent over space and time.

Distance-sampling models

The half-normal and hazard-rate key functions are robust estimating functions and allow the inclusion of covariates (Buckland et al. 1993, 2004). Therefore, we focused on these 2 key functions for the initial 2018 analysis. Our base models included no adjustments or covariates. We then added a cosine adjustment to each base model. Finally, we evaluated 2 covariates (with adjustment = NULL) for detection function g(x). The first covariate, STRATA, was used to test whether g(x) varied by deer density strata. The second covariate, COV2, was an indicator variable for tall/dense cover types (grassland, woodland, standing crop, wetland) vs short/open cover types (pasture, farmstead, harvested crop, roadsides, other). Our goal was to determine if COV2 could explain additional uncertainty in the detection function, including why g(x) might vary among strata. If COV2 could accomplish the latter, then we could pool distance data over strata to generate a more precise detection function while still generating separate density estimates for each stratum (i.e., a stratified distance-sampling estimator; Buckland et al. 1993:99–103, Miller et al. 2019). Conversely, if g(x) varied significantly by stratum, then we would need stratum-specific distance functions.

Based on what we learned in 2018, we fit all of our 2019 models using a hazard-rate function. We started by pooling the 2018 and 2019 datasets (250-m buffer surveys) and fitting some simple distance models to determine if there was evidence that g(x) varied significantly by year (annual variation), run (among-day variation), stratum, or cover type (binary indicator variable = COV2). Based on what we learned from the pooled-data analysis, we focused on fitting some simple distance models to the 2019 dataset. More specifically, we restricted our analyses to data from run 1 (similar to 2018) and used a stratified distance-sampling structure to evaluate the effect of COV2 and some new covariates that we measured in 2019 (relative topography [low, med, high], activity [lying, standing, moving], % visual obstruction [10 ordinal classes]).

Sources of variation

Temporal variation is especially important in this application. If counts and resulting population estimates are highly variable over time (within and among years), then a single-effort (non-replicated) operational survey might not be reliable. Conversely, if most of the variation in counts is due to among-PSU differences, we could address this through our sampling design (e.g., by increasing PSU sample size). We used ANOVA and linear mixed-effects methods to decompose the sampling variance of raw deer counts by PSU and run to determine if run was a significant source of variation. We also compared distance-sampling density estimates by year. Harvest and population-modeling data suggested the target population was reasonably stable during the 2-yr comparison period. Thus, we expected density estimates from distance sampling to be very similar in 2018 and 2019. Large differences in density estimates would likely reflect substantial annual variation in the observation process, which would raise questions about the reliability of the method.

Sampling-design choices

In 2018, we used a post-stratification analysis to examine an alternative stratification scheme based on a 500-m buffer and equal allocation of effort. However, in this application, the number of observations for estimating g(x) is fixed and sample allocation is confounded with the stratification scheme. Thus, a post-stratification analysis has limited utility for answering the primary question of interest: “which stratification scheme and allocation of effort will produce the most precise estimate?” Obtaining a reliable answer to this question requires a more sophisticated analysis that involves simulating the distribution of deer and detection distances in a computer-generated landscape (*sensu* Buckland et al. 2004:226–228). In 2019, we collected independent survey data from both a 250- and 500-m buffer design, which allowed us to construct simulated distance-sampling datasets (deer detections) drawn randomly from all

possible PSUs and road segments in the study area. Our focus was to examine the relative precision of the density estimates rather than to quantify bias because we did not know true density. That is, we only had estimates of 1) the distribution of perpendicular sighting distances, 2) mean encounter rate (deer groups per survey mile) and variance by stratum, and 3) mean group size and variance. We simulated the entire sampling and model-fitting process 500 times for both the 250- and 500-m buffer designs using n(PSU) = {15, 20, 25, 30} and allocation of secondary sample units (road segments) to the high stratum = {0.35, 0.50, 0.65}. We summarized the results graphically to illustrate how expected precision varied as a function of sampling-design choices.

RESULTS AND DISCUSSION

Summary Statistics

2018 (250-m buffer surveys)

We completed 48 surveys on 15 PSUs during 23 nights from 1 April to 6 May 2018. Median start time was 2058 hours (0.9 hours post-sunset) and mean survey duration was 4.1 hours. We surveyed all PSUs 3 times and we surveyed 3 PSUs 4 times. Within each PSU, we completed 3 runs within a maximum 8 days and all runs within 35 days. In total, we detected 931 deer groups (clusters) consisting of 3,194 individual deer. Of the 931 groups detected, 84% were along road segments in the high-density stratum. We observed a similar number of deer in runs 1–3 (total deer/run for all PSUs = 1,038, 1,002, and 1,082, respectively). Mean group size (observed) was 4.1 in the low-density stratum (range = 1–41, median = 3), 3.3 in the high-density stratum (range =1–42, median = 2), and 3.4 overall. Group size was not correlated with distance (r = 0.025, 95% CI = -0.039 to 0.089), which suggests we may not need an adjustment for group-size bias in our distance-sampling estimator (a common issue in distance sampling). In the low stratum, 62% of group detections were located in harvested crop fields. Conversely, only 42% of detections were in harvested crop fields in the high stratum, with relatively more detections in grasslands (24% vs. 13%) and woodlands (12% vs. 8%). For deer groups observed along low-density road segments, the mean distance to a high-strata deer-cover polygon was 446 m (median = 345 m, range = 0–2,387 m). As expected, mean perpendicular sighting distance was greater in the low stratum (135 m; range = 0–679) compared to the high stratum (108 m; range = 0–503). Additionally, the highest density of deer detections occurred ~100 m from the road (Figure 2A). We observed a similar pattern in both strata. This could result in a biased population estimate because the mean probability of detection (the area under the detection curve) can be difficult to estimate accurately if objects are not distributed randomly with respect to transect lines, as potentially indicated by a distribution of detection distances that increases rather than decreases from the transect line. This is a common and valid criticism of convenience sampling from roadways. However, if the bias is consistent over space and time, then the distance-sampling estimator might still generate a useful long-term and large-scale monitoring metric.

2019 (250-m buffer surveys)

We completed 45 surveys on 15 PSUs during 20 nights from 2 April to 2 May 2019. Median start time was 2110 hours (1.0 hours post-sunset) and mean survey duration was 3.5 hours. Within each PSU, we completed 3 runs with 2 surveys occurring a median of 1 day apart (range = 1–4) and the third survey occurring a median of 20 days (range = 10–23) after the first survey. We detected 830 deer groups (clusters) consisting of 2,710 individual deer. Of the 830 groups detected, 83% were along road segments in the high-density stratum. The total deer count increased with each run (864, 891, 955), but mean group size was similar among runs (3.4, 3.5, 2.9) and strata (3.6 in low vs. 3.2 in high). The overall group size was 3.3 deer (range = 1–21). Group size was weakly positively correlated with distance (r = 0.138, 95% CI = 0.071 to 0.204).

In the low stratum, 63% of group detections were located in harvested crop fields. Conversely, only 37% of detections were in harvested crop fields in the high stratum, with relatively more detections in grasslands (23% vs. 7%) and woodlands (12% vs. 8%). For deer groups observed along low-density road segments, the mean distance to a high-strata deer-cover polygon was 388 m (median = 254 m, range = 0–2,666). The mean perpendicular sighting distance was greater in the low stratum (136 m; range = 1–537) compared to the high stratum (109 m; range = 0–562). Similar to 2018, the distribution of detection distances increased from the road to ~100 m and then decreased (Figure 2B). We observed a similar pattern in both strata.

2019 (500-m buffer surveys)

We completed 22 surveys on 10 PSUs during 14 nights from 6 April to 3 May 2019. Median start time was 2103 hours (0.9 hours post-sunset) and mean survey duration was 3.3 hours. All PSUs were surveyed 2 times and 2 PSUs were surveyed 3 times, with the surveys occurring a median of 1 day apart (range = 1–12). We detected 318 deer groups (clusters) consisting of 1,076 individual deer. Of the 318 groups detected, 91% were along road segments in the high-density stratum. The total deer count was slightly higher for the first run (594 vs. 482), but mean group size was similar among runs (3.5 vs. 3.2) and strata (2.8 in low vs. 3.4 in high). The overall group size was 3.4 deer (range = 1–21). Group size was weakly positively correlated with distance (r = 0.148, 95% CI = 0.038 to 0.254). Compared to the 250-m buffer surveys, there were fewer meaningful differences in the distribution of deer-group observations among cover types when using the 500-m buffer. For example, 59% and 46% of group detections in the low and high strata, respectively, were located in harvested crop fields. For deer groups observed along low-density road segments, the mean distance to a high-strata deer-cover polygon was 484 m (median = 390 m, range = 0–1,945). The mean perpendicular sighting distance was greater in the low stratum (125 m; range = 29–540) compared to the high stratum (116 m; range = 0–608). Again, the distribution of detection distances increased from the road to ~100 m and then decreased (Figure 2C); the pattern was similar in both strata.

Variability in Deer Counts

Among-plot variation accounted for 80–95% of total variation in raw deer counts. Thus, variation in counts within PSUs (due to survey day) was relatively small compared to variation among PSUs. This is important because large day-to-day variation in the observation process could result in an unreliable estimator (e.g., one that is not highly repeatable). Conversely, we can address large among-plot variation through design choices such as increasing the sample of PSUs.

Model Comparisons and Density Estimates

2018 (250-m buffer, run 1)

Raw deer counts and density estimates did not vary appreciably by run. Therefore, we focused on data from run 1 (i.e., similar to an operational survey). Our top-supported model (lowest AIC) was based on the hazard-rate key function and included the COV2 covariate (Table 1). Models with STRATA as a covariate did not fit the data well, which suggests that g(x) did not vary significantly between the 2 strata. The hazard-rate detection function is described by the following equation:

$$g(x) = 1 - \exp[-(x/\sigma)^{-b}]$$

where the parameter b is a shape parameter, σ is a scale parameter, and x is the perpendicular sighting distance (which may be standardized). Covariates enter the detection function via the scale parameter (e.g., $\sigma = \beta_0 + \beta_1 COV2$). The detection function parameters from our top model were $\hat{b}$ = 1.000 (SE = 0.188), $\hat{\beta}_0$ = 4.739 (SE = 0.138), and $\hat{\beta}_1$ = 0.382 (SE = 0.141).

Given these parameters, mean detection probability was 0.602 (SE = 0.037, CV = 6.1%), which describes the area under the detection curve (e.g., Figure 3). When adjusted for the covariate COV2, the mean predicted probability of detection was 0.596 for deer located in tall/dense cover types and 0.621 for deer in short/open cover types. The density estimate from our top model was 8.2 deer/mi^2 (95% CI = 5.8–11.7; Table 1). However, density estimates from the other models were similar (Table 1). More specifically, the choice of a key function and g(x) covariates did not appreciably effect the density estimate. Likewise, the density estimates when data from each stratum were analyzed separately (not shown) were nearly identical, which supports the decision to use a stratified estimator where data are pooled across strata to estimate g(x).

Pooled data (2018 and 2019, 250-m buffer, runs 1-3)

As in 2018, the detection function g(x) varied as a function of COV2, our binary indicator variable for cover type (tall vs short). Conversely, we failed to find evidence that g(x) varied by year, run, or strata (Table 2). Models based on pooled data were not useful for predicting deer density, but helped guide the 2019 analysis.

2019 (250-m buffer, run 1)

We focused on data from run 1, which is consistent with an operational survey and our 2018 and pooled-data analyses. Our top models for 2019 included COV2, but 5 additional models had ΔAIC values <2, including the null (intercept only) model (Table 3). This may partly reflect the challenge of quantifying the suite of interacting factors that likely influence variation in the detection process (i.e., in addition to perpendicular sighting distance). This is especially true in this application because detection is based on IR imaging rather than the usual ocular process (e.g., where visual obstruction is often an important and simple detection covariate). However, more importantly, estimates of deer density did not vary appreciably among models (Table 3).

2019 (500-m buffer, run 1)

For consistency, we again focused on data from run 1 for estimating deer density. Because we had a smaller dataset (n = 10 PSUs), attempts to examine detection covariates were uninformative. Therefore, we used the COV2 model for consistency. The estimated deer density was 8.5 deer/mi^2 (95% CI = 5.5–13.2; Table 4). For a more direct comparison, we used data from the same 10 PSUs to refit the 250-m buffer model (Table 4). The estimated deer density from this model was 8.8 deer/mi^2 (95% CI = 6.1–12.7). Thus, the slightly higher density estimates probably reflect sampling variation (i.e., due to surveying a subset of PSUs).

2019 and 2020 (aerial survey)

The deer density estimates from our winter aerial surveys were both the same and equaled 6.5 deer/mi^2 (95% CI = 4.9–8.1 in 2019; 95% CI = 5.1–7.9 in 2020; MNDNR, unpublished data), which is slightly lower than distance-sampling estimates from 2018 and 2019. This is consistent with findings by others, where distance sampling tended to generate higher density estimates compared to other methods (Beaver et al. 2014, Kaminski et al. 2019). However, from a management perspective, the difference is negligible, especially if trends from these metrics are strongly positively correlated.

Expected Precision vs. Design Choices

Precision of density estimates from our 250-m buffer design were reasonably good (CV = 17–18%), but this is likely optimistic because it may not adequately reflect variation due to survey date. Not surprisingly, precision was much lower (mean CV = 25%) when we bootstrapped distance data using PSU and run (surrogate for survey date). This is probably a more realistic expectation of precision for an operational survey with a 250-m buffer, n = 15 PSUs, and

approximately equal allocation of survey effort in each stratum. A common target level of desired precision for management surveys is CV ≈ 13%. To achieve this level of precision with our current design (250-m buffer and 50:50 allocation) and assuming a single (non-replicated) operational survey would require increasing the number of PSUs from 15 to ~25. However, choices related to the stratification scheme and allocation of secondary sampling units may be important too. Our Monte Carlo simulation indicated that the 250-m buffer design with 50:50 allocation (low:high) of secondary units resulted, on average, in similar precision to the 500-m buffer design with 35:65 allocation (Figure 4). Conversely, the 250-m buffer with 35:65 allocation and the 500-m buffer with 50:50 allocation tended to produce more imprecise density estimates. Increasing the buffer distance from 250 m to 500 m resulted in approximately equal stratum weights (low = 54% of study area, high = 46% of study area), but the low stratum now had significantly fewer deer-group detections (11 vs. 39) and very low estimated densities (1.1 deer/mi^2; see Table 4). Thus, it makes sense to put more sampling effort into the high stratum to increase precision of the estimate. However, with so few deer-group observations in the low stratum, it becomes difficult to determine whether g(x) varies by stratum and one must pool data over strata to estimate g(x). Conversely, the low stratum in the 250-m buffer design is relatively large (70% of study area). Deer densities are still relatively low (3.7–4.2 deer/mi^2) in the low stratum (Table 4), but because of its size, it is important to put relatively more effort into surveying the low stratum. Thus, in the 250-m design, the 50:50 allocation generates a more precise estimate and provides more data to evaluate potential variation in g(x). However, it is important to note that we are still putting relatively more effort into the high stratum with 50:50 allocation because the high stratum only comprises 30% of the sampling frame. These tradeoffs are not necessarily straightforward. However, we now have 2 years of data from the 250-m buffer design. Therefore, for consistency, we plan to continue using the 250-m buffer design with 50:50 allocation of secondary sampling units.

CONCLUSIONS

The results from the first 2 years of the pilot study are encouraging. We identified and resolved several data collection and survey-design challenges and developed detailed field protocols to ensure consistency in data collection. Most importantly, density estimates were slightly higher but within a reasonable range of the aerial survey estimate, and annual variation in g(x) and the density estimates was negligible. Furthermore, we were able to use the first 2 years of data to explore questions about sampling-design tradeoffs. Another year of data collection on the same study area will strengthen our inferences and help determine if 1) g(x) and the distribution of deer relative to roads and cover is relatively consistent over time and space, and 2) the effect of variation in spring dispersal can be minimized by using observational cues to inform the start of the survey.

ACKNOWLEDGMENTS

We thank M. Diamond, G. Gehring, E. Jones, T. Klinkner, M. Orr, A. Strzelczyk, B. Wagner, and J. Westfield for conducting the surveys. N. Davros reviewed an earlier draft of this report. This project was funded in part by the Wildlife Restoration (Pittman-Robinson) Program.

LITERATURE CITED

Anderson, D. R., J. L. Laake, B. R. Crain, and K. P. Burnham. 1979. Guidelines for line transect sampling of biological populations. Journal of Wildlife Management 43:70–78.

Beaver, J. T., C. A. Harper, R. E. Kissell Jr, L. I. Muller, P. S. Basinger, M. J. Goode, F. T. Van Manen, W. Winton, and M. L. Kennedy. 2014. Aerial vertical-looking infrared imagery to evaluate bias of distance sampling techniques for white-tailed deer. Wildlife Society Bulletin 38:419–427.

Buckland, S. T., D. R. Anderson, K. P. Burnham, and J. L. Laake. 1993. Distance sampling: estimating abundance of biological populations. Chapman and Hall, London, reprinted 1999 by RUWPA, University of St. Andrews, Scotland.

Buckland, S. T., D. R. Anderson, K. P. Burnham, J. L. Laake, D. L. Borchers, and L. Thomas. 2004. Advanced distance sampling: estimating abundance of biological populations. Oxford University Press, Oxford, United Kingdom.

Burnham, K. P., D. R. Anderson, and J. L. Laake. 1980. Estimation of density from line transect sampling of biological populations. Wildlife Monographs 72.

Collier, B. A., S. S. Ditchkoff, J. B. Raglin, and J. M. Smith. 2007. Detection probability and sources of variation in white-tailed deer spotlight surveys. Journal of Wildlife Management 71:277–281.

DeYoung, C. A. 2011. Population dynamics. Pages 147–180 *in* D. G. Hewitt, editor. Biology and management of white-tailed deer. CRC Press, Boca Raton, Florida, USA.

Focardi, S., A. M. De Marinis, M. Rizzotto, and A. Pucci. 2001. Comparative evaluation of thermal infrared imaging and spotlighting to survey wildlife. Wildlife Society Bulletin 29:133–139.

Gasaway, W. C., S. D. Dubois, D. J. Reed, and S. J. Harbo. 1986. Estimating moose population parameters from aerial surveys. Biological Papers of the University of Alaska 22, Fairbanks, Alaska, USA.

Haroldson, B. S., R. G. Wright, and C. Pouliot. 2015. DNRSurvey User Guide 2.30.01. <http://www.dnr.state.mn.us/mis/gis/DNRSurvey/DNRSurvey.html>.

Kaminski, D. J., T. M. Harms, and J. M. Coffee. 2019. Using spotlight observations to predict resource selection and abundance for white-tailed deer. Journal of Wildlife Management 83:1565–1580.

Marques, T. A., S. T. Buckland, R. Bispo, and B. Howland. 2013. Accounting for animal density gradients using independent information in distance sampling surveys. Statistical Methods and Applications 22:67–80.

Marques, T. A., S. T. Buckland, D. L. Borchers, D. Tosh, and R. A. McDonald. 2010. Point transect sampling along linear features. Biometrics 66:1247–1255.

McCullough, D. L. 1982. Evaluation of night spotlighting as a deer study technique. Journal of Wildlife Management 46:963–973.

McShea, W. J., C. M. Stewart, L. Kearns, and S. Bates. 2011. Road bias for deer density estimates at 2 national parks in Maryland. Wildlife Society Bulletin 35:177–184.

Miller, D. L., E. Rexstad, L. Tomas, L. Marshall, and J. L. Laake. 2019. Distance sampling in R. Journal of Statistical Software 89:1–28.

Mitchell, W. A. 1986. Deer spotlighting census: section 6.4.3, U.S. Army Corp of Engineers wildlife resources management manual. U.S. Army Engineer Waterways Experiment Station Technical Report EL–86–53, Vicksburg, Mississippi, USA.

R Core Team. 2020. R: A language and environment for statistical computing. R Foundation for Statistical Computing, Vienna, Austria. <https://www.R-project.org/>, accessed 15 May 2020.

Stainbrook, D. P. 2011. Methods of estimating white-tailed deer abundance at Gettysburg National Military Park: testing assumptions of distance sampling. Thesis, School of Forest Resources, Pennsylvania State University, University Park, USA.

Stevens, D. L. Jr., and A. R. Olsen. 2004. Spatially balanced sampling of natural resources. Journal of the American Statistical Association 99:262–278.

Table 1. Distance sampling models used to evaluate roadside surveys of white-tailed deer in southern Minnesota, fit to the 2018 dataset. Data were collected during April and early May. For all models, we restricted survey data to the initial run (replicate) of the 15 primary sampling units, after right truncation (300 m). Analysis was restricted to the half-normal (HN) and hazard-rate (HR) key functions. Covariates included deer density strata (STRATA = low, high) and tall (i.e., grassland, woodland, standing crops, wetland) vs short (i.e., pasture, farmstead, harvested crops, roadsides, other) cover types (COV2). Number of model parameters (K), Akaike's Information Criterion (AIC) values, change in AIC values relative to the top model (ΔAIC), AIC weights (ω), log likelihood (LL), density estimates (deer/mi^2), and 95% confidence intervals (CI) are also presented.

Model	Key function	Covariates	K	AIC	ΔAIC	ω	LL	Density	95% CI
M7	HR	~COV2	3	3103.0	0.0	0.815	-1548.5	8.2	5.8-11.7
M8	HR	~STRATA	3	3107.1	4.1	0.106	-1550.5	8.1	5.7-11.6
M5	HR	~1	2	3109.1	6.1	0.039	-1552.5	8.3	5.7-12.0
M3	HN	~COV2	2	3110.1	7.1	0.023	-1553.1	8.6	6.1-12.3
M6	HR+Cos2	~1	3	3111.1	8.1	0.014	-1552.5	8.3	5.3-13.0
M2	HN+Cos2	~1	2	3115.9	12.9	0.001	-1555.9	8.0	5.3-12.0
M1	HN	~1	1	3116.2	13.2	0.001	-1557.1	8.7	6.1-12.5
M4	HN	~STRATA	2	3116.4	13.4	0.001	-1556.2	8.5	6.0-12.1

Table 2. Distance sampling models used to evaluate roadside surveys of white-tailed deer in southern Minnesota, fit to the 2018-2019 pooled dataset. Data were collected during April and early May. For all models, we restricted data to the 250-m buffer surveys, after right truncation (300 m). Analysis was restricted to the hazard-rate (HR) key function. Covariates included year (YEAR), survey replicate (RUN), deer density strata (STRATA = low, high), and tall (i.e., grassland, woodland, standing crops, wetland) vs short (i.e., pasture, farmstead, harvested crops, roadsides, other) cover types (COV2). Number of model parameters (K), Akaike's Information Criterion (AIC) values, change in AIC values relative to the top model (ΔAIC), AIC weights (ω), and log likelihood (LL) are also presented.

Model	Key function	Covariates	K	AIC	ΔAIC	ω	LL
P5	HR	~COV2	3	17930	0.0	0.999	-8962.0
P4	HR	~STRATA	3	17945	14.5	0.001	-8969.3
P1	HR	~YEAR	3	17960	30.4	0.000	-8977.2
P2	HR	~RUN	4	17961	30.5	0.000	-8976.3
P0	HR	~1	2	17961	30.9	0.000	-8978.4
P3	HR	~YEAR * RUN	7	17963	33.4	0.000	-8974.7

Table 3. Distance sampling models used to evaluate roadside surveys of white-tailed deer in southern Minnesota fit to the 2019 dataset. Data were collected during April and early May. For all models, we restricted survey data to the initial run (replicate) of the 15 primary sampling units of the 250-m surveys, after right truncation (300 m). Analysis was restricted to the hazard-rate (HR) key function. Covariates included tall (i.e., grassland, woodland, standing crops, wetland) vs short (i.e., pasture, farmstead, harvested crops, roadsides, other) cover types (COV2), relative topography (TOPO = low, medium, high), deer activity (ACTIVITY = lying, standing, moving), and % visual obstruction class (OBSTR). Number of model parameters (K), Akaike's Information Criterion (AIC) values, change in AIC values relative to the top model (ΔAIC), AIC weights (ω), log likelihood (LL), density estimates (deer/mi^2), and 95% confidence intervals (CI) are also presented.

Model	Key function	Covariates	K	AIC	ΔAIC	ω	LL	Density	95% CI
M1	HR	~COV2	3	2647.5	0.0	0.219	-1320.7	8.0	5.7-11.3
M6	HR	~COV2+TOPO	5	2648.2	0.7	0.155	-1319.1	8.1	5.7-11.5
M7	HR	~COV2+ACTIVITY	5	2648.5	1.1	0.130	-1319.3	8.1	5.7-11.4
M2	HR	~1	2	2649.3	1.8	0.088	-1322.6	8.0	5.6-11.5
M8	HR	~COV2+OBSTR	4	2649.3	1.9	0.087	-1320.7	8.0	5.7-11.3
M5	HR	~COV2+TOPO+ACTIVITY	7	2649.3	1.9	0.085	-1317.7	8.1	5.7-11.5
M9	HR	~TOPO	4	2650.0	2.5	0.061	-1321.0	8.1	5.6-11.7
M4	HR	~COV2+TOPO+OBSTR	6	2650.1	2.7	0.058	-1319.1	8.1	5.7-11.5
M11	HR	~ACTIVITY	4	2650.4	2.9	0.051	-1321.2	8.1	5.7-11.5
M3	HR	~COV2+TOPO+OBSTR+ACTIVITY	8	2651.2	3.8	0.033	-1317.6	8.1	5.7-11.5
M10	HR	~OBSTR	3	2651.3	3.8	0.033	-1322.6	8.0	5.6-11.5

Table 4. Top distance sampling models by year and buffer size used to evaluate roadside surveys of white-tailed deer in southern Minnesota, spring 2018 and 2019. For all models, we restricted survey data to the initial run (replicate) of the 10 or 15 primary sampling units (PSU), after right truncation (300 m). Summary statistics include number of PSU, stratum weight (proportion of study area defined as low deer density [Wt (L)]), transect length (Tran [mi]) by deer density strata (L=low, H=high), number of deer groups observed (Groups) by strata, mean detection probability (P), density estimates (deer/mi^2) by strata, 95% confidence intervals (CI), and coefficient of variation(CV).

Year	Buffer (m)	PSU	Wt (L)	Tran (L)	Tran (H)	Groups (L)	Groups (H)	g(x)	P	Density (L)	Density (H)	Density (Total)	95% CI	CV (%)
2018	250	15	0.70	196	193	46	234	HR(COV2)	0.602	3.7	19.0	8.2	5.8-11.7	17.6
2019	250	15	0.70	196	189	50	191	HR(COV2)	0.537	4.1	17.2	8.0	5.7-11.3	17.1
2019	250	10	0.70	135	130	39	155	HR(COV2)	0.558	4.2	19.7	8.8	6.1-12.7	17.8
2019	500	10	0.54	139	144	11	143	HR(COV2)	0.532	1.1	17.2	8.5	5.5-13.2	20.1

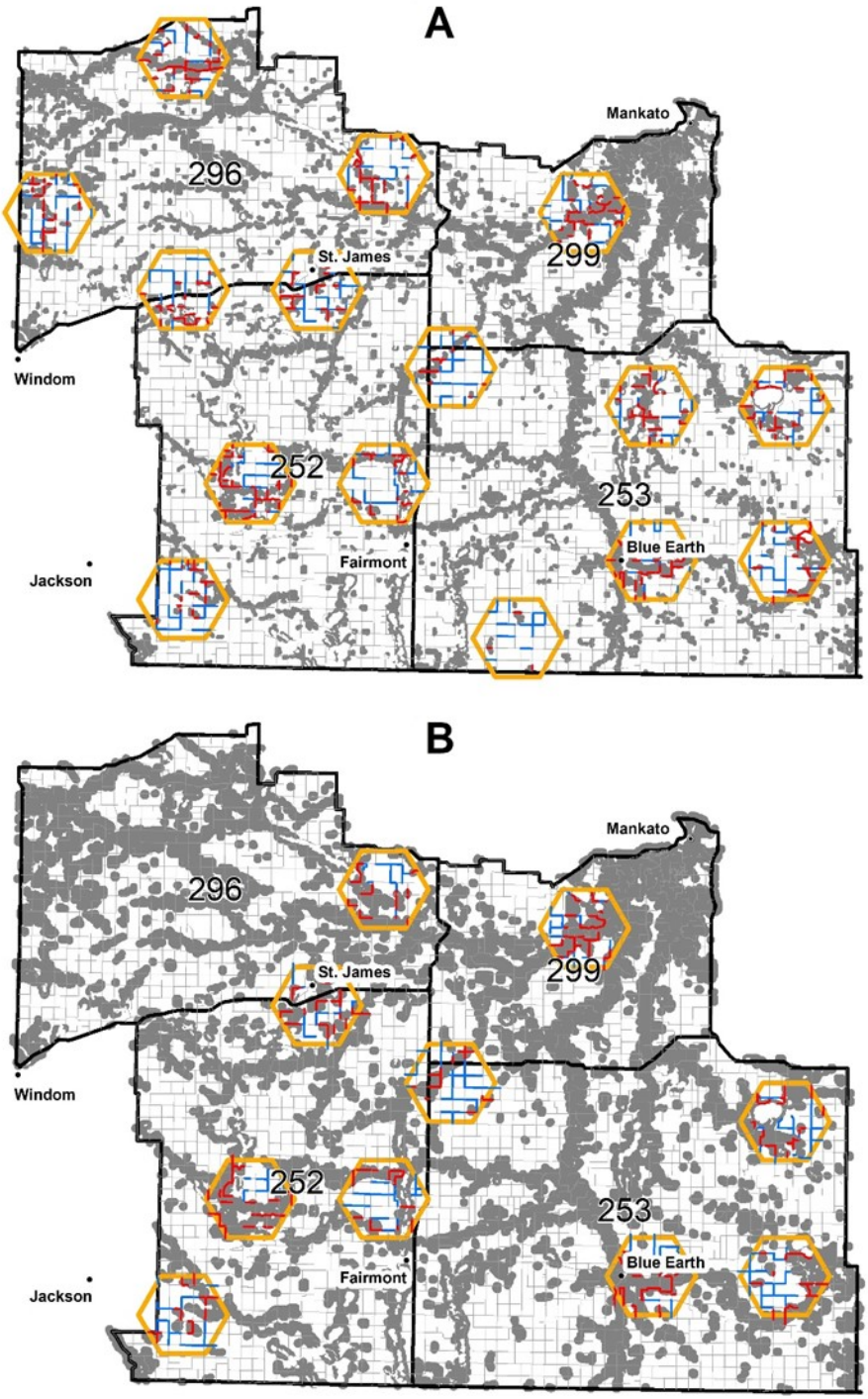

Figure 1. Sampling frame (deer permit areas 252, 253, 296, 299), primary sampling units (PSU; hexagons), and secondary sampling units (road segments; red = high-density stratum, blue = low-density stratum) for roadside distance-sampling surveys of white-tailed deer in southern Minnesota during **A**) spring 2018 and 2019 (250-m buffer surveys) and **B**) spring 2019 (500-m buffer surveys). Grey areas denote deer-cover polygons (≥2 ac) consisting of woodland, grassland, and wetland cover types with a 250-m or 500-m buffer.

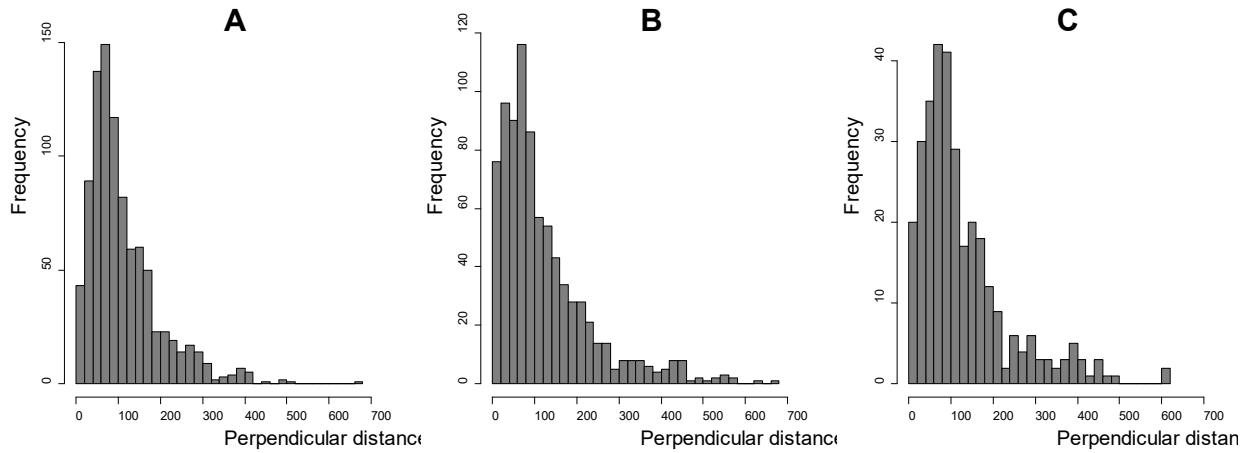

Figure 2. Distribution of perpendicular sighting distances from roadside distance-sampling surveys of white-tailed deer in southern Minnesota during **A**) spring 2018 (250-m buffer surveys), **B**) spring 2019 (250-m buffer surveys), and **C**) spring 2019 (500-m buffer surveys). Data include distance measurements collected during 2–4 replicate surveys of 10–15 primary sampling units.

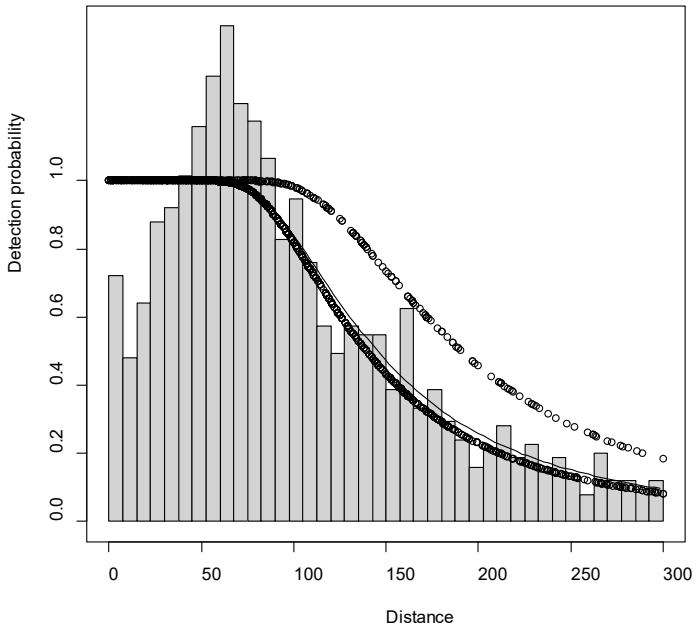

Figure 3. Estimated detection function from our top pooled distance-sampling model overlaid on a histogram of deer-group observations as a function of perpendicular sighting distance during roadside surveys of white-tailed deer in southern Minnesota, spring 2018 and 2019. The solid curved line denotes the average detection function. The lower line of circles denotes the detection curve for deer groups observed in tall/dense cover types (grassland, woodland, standing crops, wetland) and the upper line of circles denotes the detection curve for deer groups observed in short/open cover types (pasture, farmstead, harvested crops, roadsides, other).

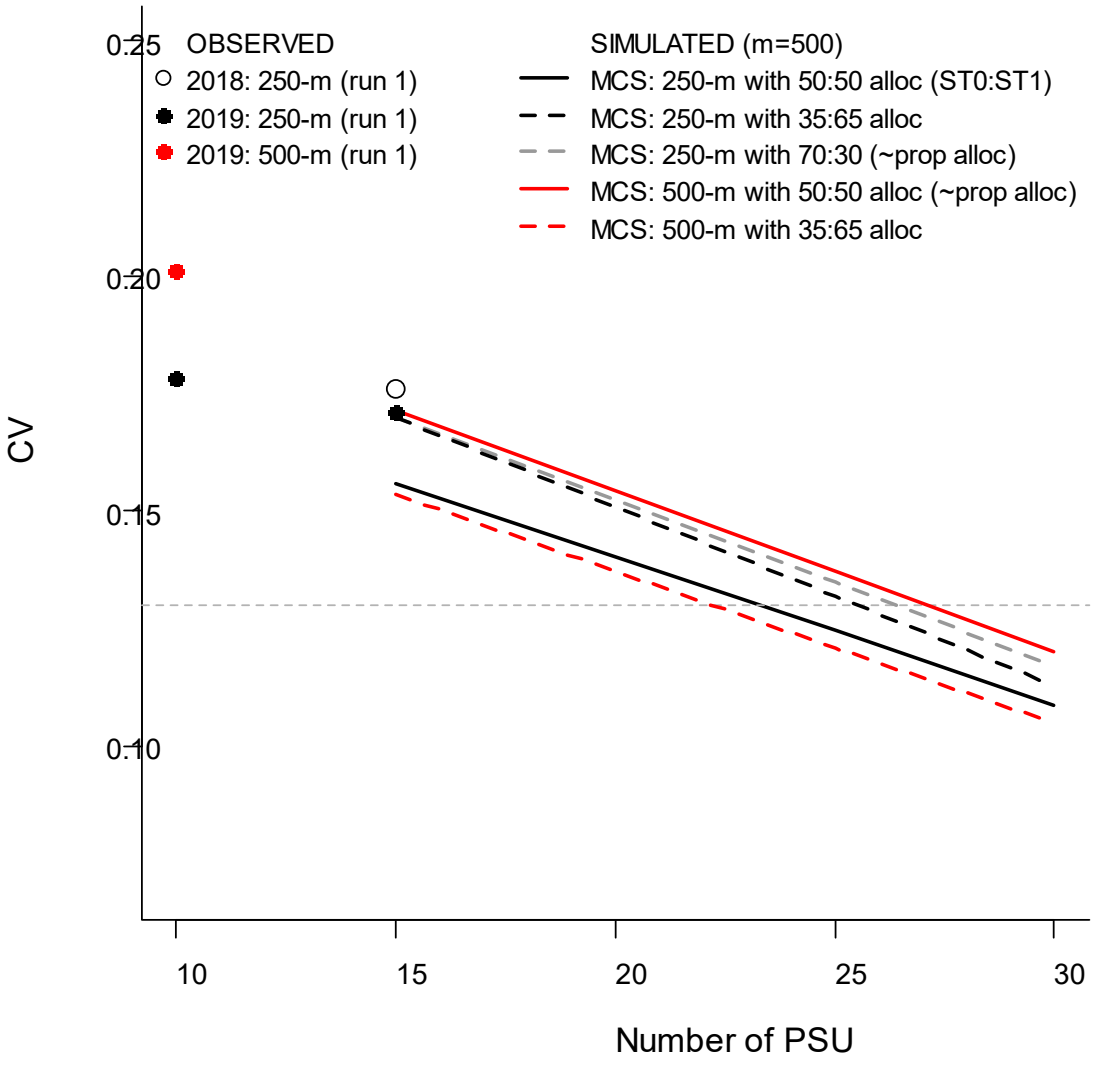

Figure 4. Expected precision of population estimates as a function of sample size (number of primary sampling units; PSU), stratification scheme (250- vs. 500-m buffer around deer-habitat polygons), and allocation of secondary sampling units (road segments) to strata. Estimates were derived from a Monte Carlo simulation with 500 replicates based on data from roadside distance-sampling surveys of white-tailed deer in southern Minnesota, spring 2018 and 2019. The gray dashed horizontal line denotes a common target level of precision for management surveys.